

## WATER WAVES IN VARIABLE DEPTH UNDER CONTINUOUS SEA ICE

James T. Kirby  
 University of Delaware  
 Newark, Delaware, USA

### Abstract

An extension to the linear mild-slope approximation for surface water waves which accounts for the effect of a continuous cover of floating ice is developed. The ice is allowed to have spatially slowly varying properties, such as thickness, elasticity and in-plane compression, while the water column has variable finite depth and may be slowly moving. Results are given for refracting and shoaling waves over planar topography. A parabolic approximation for combined refraction-diffraction is used to study several example problems.

**key words:** sea ice, surface waves, wave models, wave propagation

### 1 Introduction

A continuous ice cover has a marked effect on the properties of wind waves in coastal regions during the winter season. To date, most analytic studies of the behavior of waves under ice have concentrated on deep water phenomena, or have considered restricted classes of motion in shallow water for which analytic results are simply obtained. In this study, a new framework is provided for studying progressive water waves under ice in water of finite depth. The model described here retains the usual effects included in the mild-slope approximation for surface waves (Kirby, 1984): slowly varying depth, slowly varying ambient current, and full frequency dispersion. In addition, the new model accounts for a continuous ice cover, and can account for the effects of slowly varying ice thickness and slowly varying in-plane compression forces. The resulting model provides a unifying framework for all previously obtained geometric optics results, and allows for the development of the parabolic approximation in order to study combined refraction-diffraction.

A derivation of the governing equations is provided first. Then, the refraction approximation is obtained, and several simple results following from Snell's law are presented. We then describe a parabolic equation and show several results which indicate the types of effects to be expected.

### 2 Derivation of the linearized wave model

The governing wave equations are obtained by means of Hamilton's variational principle, using an un-averaged Lagrangian. Hamilton's principle is given by

$$\delta \int_{\mathbf{x}} \int_t L dt dx = 0, \quad (1)$$

which indicates that the integral of a Lagrangian  $L$  over the propagation space  $(\mathbf{x}, t)$  is stationary with respect to variations of the unknown dependent variables determining  $L$ . Here,  $\mathbf{x}$  is a horizontal coordinate system taken to lie in the plane of the still water surface. Luke (1967) showed that taking  $L$  to be the integral over depth of the fluid pressure allows for the complete specification of the boundary value problem for inviscid, irrotational wave motion with no surface tension. Using Bernoulli's equation, we may write

$$L = \int_{-h}^{\eta} p dz = -\rho \int_{-h}^{\eta} \left\{ gz + \phi_t + \frac{1}{2}(\nabla\phi)^2 \right\} dz \quad (2)$$

where  $\nabla$  denotes a gradient operator in 3-space.

The formulation of Luke was further extended by Simmons (1969) to include the effect of surface tension. We now consider adding a continuous ice layer to the fluid column. The ice has density  $\rho_i < \rho$ , thickness  $d$ , elastic modulus  $E$  and Poisson ratio  $\nu$ . We define a stiffness  $D$  by

$$D = \frac{Ed^3}{12(1-\nu^2)} \quad (3)$$

We also consider an in-plane stress in the ice, characterized by the stress tensor  $T_{ij}$ , which may also vary slowly in space.

The Lagrangian is extended by adding the appropriate kinetic and potential energy terms to the  $L_w$  form, giving

$$\begin{aligned} L_i &= L_w + K_i - V_i \\ &= L_w + \frac{\rho_i d}{2} (\eta_t)^2 - \frac{T_{ij}}{2} \frac{\partial \eta}{\partial x_i} \frac{\partial \eta}{\partial x_j} - \frac{D}{2} \\ &\quad [(\nabla_h^2 \eta)^2 - 2(1-\nu)(\eta_{xx}\eta_{yy} - \eta_{xy}^2)] \end{aligned} \quad (4)$$

where  $K_i, V_i$  denote the kinetic energy and potential energy associated with the ice. The added terms denote, in order, the kinetic energy associated with the vertical motion of the ice, the change in potential energy of the fluid resulting from work done against the in-plane stress of the ice plate, and the change in potential energy

associated with the bending energy of the ice plate (Love, 1944, section 329). We retain only small displacement approximations. We will also restrict our attention here to isotropic in-plane compression of the ice with compression force  $T$ ;  $T_{i,j} = -T\delta_{ij}$ . The compression force may be thought of simply as the opposite of the tensile force appearing in the surface tension problem.

It will be of some use below to have estimates of the size of several of the terms in the Lagrangian. We introduce scaled variables by choosing  $k^{-1}$  as a length scale for spatial derivatives and  $a$  as an amplitude scale for the vertical surface displacement. In order for the gravity restoring effects to give a reference  $O(1)$  contribution to the wave motion, we choose  $\phi_0 = a\sqrt{g/k}$  as the scale for  $\phi$  and  $(\sqrt{gk})^{-1}$  as the scale for time. Dividing the Lagrangian by  $\rho g a^2$  then gives the dimensionless form

$$L = -\frac{1}{2}\eta^2 - \int_{-kh}^{k\eta} \left[ \phi_t + \frac{1}{2}(\nabla\phi)^2 \right] dz + \frac{\lambda_1}{2}(\nabla_h\eta)^2 - \frac{\lambda_2}{2}(\nabla_h^2\eta)^2 + \frac{1}{2}\frac{\rho_i}{\rho}kd(\eta_h)^2 \quad (5)$$

where the dimensionless parameters  $\lambda_1$  and  $\lambda_2$  are given by

$$\lambda_1 = \frac{Tk^2}{\rho g} \quad (6)$$

$$\lambda_2 = \frac{Dk^4}{\rho g} \quad (7)$$

The two  $\lambda$  parameters characterize the relative importance of in-plane stress and bending stress as loads on the water column, relative to the gravitational effect. These may be small or large relative to the gravity terms depending on the stiffness of the ice, the amount of in-plane stress, and the wavelength or wave frequency. On the other hand, the vertical kinetic energy term is characterized by the parameter  $kd$ , which represents the ratio of ice thickness to wave length. This ratio is small for most cases of interest.

## 2.1 The linear wave model

The leading order approximation for linearized wave motion is now obtained. Including the effect of a slowly varying but possibly large current under the ice, we may write the velocity potential  $\phi$  as

$$\phi = \int \mathbf{U} \cdot d\mathbf{x} + f(z)\bar{\phi}(\mathbf{x}, t), \quad (8)$$

where  $\mathbf{U}(\mathbf{x})$  is the imposed, uniform-over-depth current field,  $\bar{\phi}$  is the value of the potential at the mean water level, and

$$f(z) = \frac{\cosh k(h+z)}{\cosh kh} \quad (9)$$

The quantities  $\bar{\phi}$  and  $\eta$  are then regarded as the unknown dependent variables to be obtained in a solution. Retaining terms which are quadratic in the unknowns in  $L$  leads to

$$L_i = -\rho\eta\bar{\phi}_t - \rho\eta\mathbf{U} \cdot \nabla_h\bar{\phi} - \frac{\rho g\eta^2}{2} - \frac{\rho}{2}F_1(\nabla_h\bar{\phi})^2 - \frac{\rho}{2}F_2\bar{\phi}^2 + \frac{\rho_i d}{2}(\eta_t)^2 + \frac{T}{2}(\nabla_h\eta)^2 - \frac{D}{2}[(\nabla_h^2\eta)^2 - 2(1-\nu)(\eta_{xx}\eta_{yy} - \eta_{xy}^2)] \quad (10)$$

where

$$F_1 = \int_{-h}^0 f^2 dz = \frac{\tanh kh}{2k} \left( 1 + \frac{2kh}{\sinh 2kh} \right) \quad (11)$$

$$F_2 = \int_{-h}^0 (f_z)^2 dz = \frac{k \tanh kh}{2} \left( 1 - \frac{2kh}{\sinh 2kh} \right) \quad (12)$$

In the absence of an ice layer, the dispersion relation for surface waves is given by

$$\omega = \sigma + \mathbf{k} \cdot \mathbf{U}; \quad \sigma^2 = gk \tanh kh \quad (13)$$

and we obtain

$$F_1 = \frac{CC_g}{g}; \quad F_2 = \frac{(\sigma^2 - k^2 CC_g)}{g} \quad (14)$$

where  $C = \sigma/k$  is the phase speed relative to the current and  $C_g = \partial\sigma/\partial k$  is the relative group velocity. With the tension and bending effects included, these integrals do not have simple physical interpretations.

The desired governing equations follow by taking variations of  $L_i$  with respect to the unknowns  $\eta$  and  $\bar{\phi}$ . Variation with respect to  $\eta$  under the integral (1) and partial integration leads to the Euler-Lagrange equation

$$\frac{D\bar{\phi}}{Dt} + g\eta + \frac{\rho_i}{\rho}d\eta_{tt} + \nabla_h \cdot \left( \frac{T}{\rho} \nabla_h \eta \right) + \nabla_h^2 \left( \frac{D}{\rho} \nabla_h^2 \eta \right) + \frac{\epsilon}{\rho} = 0. \quad (15)$$

The operator  $D/Dt$  represents a total derivative following the current  $\mathbf{U}$ . We allow for slow variations in ice properties by allowing  $D$  and  $T$  to vary as functions of  $\mathbf{x}$ . The last term is a small quantity which evaluates to

$$\epsilon = 2\gamma_{xy}\eta_{xy} - \gamma_{xx}\eta_{yy} - \gamma_{yy}\eta_{xx}; \quad \gamma = D(1-\nu) \quad (16)$$

We neglect  $\epsilon$  from here on since the remainder of the derivation above explicitly neglects second-order small terms in the problem for the fluid column (Kirby, 1984). A number of authors have obtained various forms of (15), starting with Greenhill (1887). The form of the equation with variable ice stiffness is essentially similar to an equation given by Krasil'nikov (1962), but with the inclusion of additional current, compression and acceleration effects.

For the case of constant water depth, the term involving  $\bar{\phi}$  in (15) is usually handled by substituting the expression for the constant depth solution. For the case of a slowly varying depth, we proceed by taking variations of  $L_i$  with respect to  $\bar{\phi}$ , which leads to the Euler-Lagrange equation

$$\frac{D\eta}{Dt} + (\nabla_h \cdot \mathbf{U})\eta = -\nabla_h \cdot (F_1 \nabla_h \bar{\phi}) + F_2 \bar{\phi} \quad (17)$$

This is basically a kinematic constraint on the fluid column. In the presence of ice and current, it is likely that the simplest approach is to treat (15) and (17) as a set of coupled equations. In the absence of a current, the total derivative appearing in (15) and (17) reduces to a partial derivative with respect to time, and the two equations can be collapsed more simply. The simplest general system results from eliminating  $\bar{\phi}$  between (15) and (17), giving

$$\eta_{tt} + \{F_2 - \nabla_h \cdot (F_1 \nabla_h (\cdot))\} [g\eta + \frac{\rho_i d}{\rho} \eta_{tt} + \nabla_h \cdot \left( \frac{T}{\rho} \nabla_h \eta \right) + \nabla_h^2 \left( \frac{D}{\rho} \nabla_h^2 \eta \right)] = 0 \quad (18)$$

No simple generalization to a single-variable equation has been found for the case where currents are retained.

## 2.2 Plane wave solutions

The plane wave solutions for the system described here are well known from previous studies; they are described here in order to establish notation for subsequent sections and to check the validity of the equations. For the case of a domain with constant parameters, we introduce the expressions

$$\eta = ae^{i\psi}; \quad \bar{\phi} = -iAe^{i\psi} \quad (19)$$

where  $a$  and  $A$  are constant real amplitudes and  $\psi$  is a phase function. We further introduce

$$\mathbf{k} = \nabla_h \psi; \quad \omega = -\psi_t \quad (20)$$

as definitions for the wavenumber vector and wave frequency. Using (19) in (15) and (17) and neglecting ice acceleration effects leads to the expressions

$$A = \frac{g\sigma a}{\sigma_0^2} \quad (21)$$

and

$$\sigma = \omega - \mathbf{k} \cdot \mathbf{U}; \quad \sigma^2 = \sigma_0^2(1 - \lambda_1 + \lambda_2) \quad (22)$$

with

$$\sigma_0^2 = gk \tanh kh \quad (23)$$

In the absence of an ice layer, (22) and (23) reduce to (13), the dispersion relation for wave-current interaction with a free surface.

An expression for the group velocity vector may be obtained according to

$$\mathbf{C}_g = \frac{\partial \omega}{\partial \mathbf{k}} = \mathbf{U} + \frac{\partial \sigma}{\partial \mathbf{k}} \quad (24)$$

We denote

$$C_{gr} = \frac{\partial \sigma}{\partial k} \quad (25)$$

as the scalar group velocity relative to the moving domain, and obtain the expression

$$C_{gr} = \frac{\sigma}{2k} \left( 1 + \frac{2kh}{\sinh 2kh} \right) + \frac{\sigma_0^2}{\sigma k} (2\lambda_2 - \lambda_1) \quad (26)$$

Finally, an expression for the local average energy density is given by

$$\rho E = \frac{1}{2} \rho g a^2 (1 - \lambda_1 + \lambda_2) = \frac{1}{2} \rho g a^2 \left( \frac{\sigma}{\sigma_0} \right)^2 \quad (27)$$

Note that the expression for  $\sigma^2$  in (22) may become negative if the in-plane compression force acting on the ice becomes sufficiently large. Under this condition, the ice layer becomes unstable, and it is usually assumed that a local fracture of the ice would result. We note here that the effect can be related to the fact that the Hamiltonian density is not positive definite, with the instability occurring when the energy density takes on values which are negative relative to an undisturbed surface. The effect of in-plane compression on the wave dispersion relation was described by Kheisin (1967), and has been more thoroughly investigated more recently by a number of authors starting with Kerr (1983). Schulkes et al (1987) suggest that values of  $T$  occurring in the field would not be expected to lead either to the instability of the ice layer, or to a negative or zero value of  $C_{gr}$  in (26). However, Liu and Mollo-Christensen (1988) have suggested that compression effects are prominent in the field, and provided an analysis that suggests that the local reduction in group velocity can lead to large wave events observed in the Weddell Sea. The effect of in-plane stress may thus significantly modify values of the parameters in the dispersion relation under normal conditions, and should be carefully considered.

### 2.3 Equation for long waves

For waves which are long relative to the depth of water,  $kh$  takes on small values and the coefficients in (11)-(12) approach the limits

$$F_1 \rightarrow h; \quad F_2 \rightarrow 0 \quad (28)$$

In this limit, water depth can become comparable to (or less than) ice thickness, and it is usually appropriate to retain the ice acceleration effects in short wind waves are being considered. In this limit, and neglecting current effects, the equations may be combined to give

$$\eta_{tt} - \nabla_h \cdot \left[ h \nabla_h \left( \frac{\rho_i}{\rho} d\eta_{tt} \right) \right] = \nabla_h \cdot \left[ g h \nabla_h (\eta + \nabla_h \cdot \left( \frac{T}{\rho g} \nabla_h \eta \right) + \nabla_h^2 \left( \frac{D}{\rho g} \nabla_h^2 \eta \right) \right]. \quad (29)$$

For the case  $D = 0$  and all other coefficients constant, the resulting model is equivalent to the model described in Keller and Goldstein (1953). Here, the variable coefficient extension for the shallow water model appears as the appropriate limit of the more general mild-slope model obtained above.

## 3 The refraction approximation

We now consider the equations governing the variation of a wave train in a slowly modulated domain. We will first obtain a coupled eikonal - transport model which retains diffraction effects. We will then drop the diffraction terms to arrive at a geometric optics approximation, as in Keller (1958) and Bretherton and Garrett (1969). Results for Snell's law shoaling on a plane beach are then presented.

### 3.1 Eikonal - transport equations

We start from the pair of equations (18) and (20) with the ice acceleration term dropped. Since the equations may not be combined in a straightforward manner, we adopt the expressions:

$$\eta = ae^{i\psi}, \quad \tilde{\phi} = -iAe^{i\psi} \quad (30)$$

where now  $a$  and  $A$  are real amplitudes which vary slowly in space and time, and  $\psi$  is a real phase function. We also take

$$\mathbf{K} = \nabla_h \psi, \quad \omega = -\psi_t \quad (31)$$

The first expression guarantees that

$$\nabla_h \times \mathbf{K} = 0 \quad (32)$$

which can be used to obtain  $\mathbf{K}$  when used together with an eikonal equation. The leading order solution for  $A$  may be written as

$$A = \frac{g\sigma^*}{\sigma_0^2} a \quad (33)$$

Using (30)-(33) in (15) and (17) leads to a complicated expression containing a real and imaginary part. Since the amplitudes and phase functions are assumed to be real quantities, we separate the parts and obtain

$$\left[ \frac{E}{\sigma} \left( \frac{\sigma^*}{\sigma} \right) \right]_t + \nabla_h \cdot \left[ \frac{E}{\sigma} \left( \frac{\sigma^*}{\sigma} \mathbf{U} + \left( \frac{\sigma^*}{\sigma} \right)^2 C_{g1} \frac{\mathbf{K}}{k} + (2\lambda_2^* - \lambda_1^*) \frac{\sigma_0^2}{\sigma} \frac{\mathbf{K}}{|\mathbf{K}|^2} \right) \right] = 0 \quad (34)$$

and

$$\left( \frac{\sigma^*}{\sigma_0} \right)^2 \left\{ 1 - \frac{C_{g1}}{\sigma k} (|\mathbf{K}|^2 - k^2) + \frac{1}{\sigma^* a} \nabla_h \cdot \left[ \frac{ig m a_0^2 C_{g1}}{\sigma k} \nabla_h \left( \frac{\sigma^* a}{\sigma_0^2} \right) \right] \right\} - (1 - \lambda_1^* + \lambda_2^*) - \frac{1}{a} \nabla_h \cdot \left( \frac{\lambda_1^*}{|\mathbf{K}|^2} \nabla_h a \right) - \frac{D(a)}{ga} = 0. \quad (35)$$

where

$$C_{g1} = \frac{\sigma}{2k} \left( 1 + \frac{2kh}{\sinh 2kh} \right) \quad (36)$$

(34) and (35) are the action transport equation and the eikonal equation, respectively. These equations may be used as the basis for a combined refraction-diffraction calculation by solving (35) for the scalar  $|\mathbf{K}|$ , (32) for the direction of  $\mathbf{K}$ , and (34) for the action  $E/\sigma$ .

### 3.2 The geometric optics limit

The geometric optics approximation may be obtained by neglecting diffraction effects in the eikonal-transport model (34)-(35). In this limit, all starred quantities in the previous sections reduce to their plane wave approximations, given in section 2.2. We are left with (32) together with

$$|\mathbf{K}|^2 = k^2; \quad \sigma^2 = \sigma_0^2(1 - \lambda_1 + \lambda_2), \quad (37)$$

which completely determines the wavenumber and wave direction. The transport equation reduces to

$$\left(\frac{E}{\sigma}\right)_t + \nabla_h \cdot \left(\frac{E}{\sigma} \mathbf{C}_g\right) = 0. \quad (38)$$

where the group velocity vector is described in (24). This result is completely analogous to the action conservation principle developed by Bretherton and Garrett (1969). Any available refraction scheme used to study the wave-current-variable depth case may be simply extended to include the effects described here by a suitable redefinition of the group velocity and dispersion relation.

### 3.3 Refraction and shoaling over a plane slope

For the case of waves approaching shore over a one-dimensional topography  $h(x)$ , the results above can be greatly simplified. Denoting  $\theta$  as the angle between the local direction of propagation and the  $x$  axis and imposing conservation of wave crests in the  $y$  direction, we obtain the relation

$$k \sin \theta = k_0 \sin \theta_0 \quad (39)$$

or Snell's law. Subscripts 0 denote deepwater conditions. For the case where wave height does not vary in the longshore direction (and in the absence of currents and time variations), (38) reduces to

$$\frac{E}{\sigma} C_{gr} \cos \theta = \text{constant} \quad (40)$$

Using the expression (27) for the wave energy and rearranging, we obtain

$$\frac{a}{a_0} = K_s K_r \quad (41)$$

where  $K_s$  is the shoaling coefficient given by

$$K_s = \left(\frac{C_{gr0}}{C_{gr}}\right)^{1/2} \left(\frac{1 - \lambda_{10} + \lambda_{20}}{1 - \lambda_1 + \lambda_2}\right)^{1/2} \quad (42)$$

and  $K_r$  is the refraction coefficient given by

$$K_r = \left(\frac{\cos \theta_0}{\cos \theta}\right)^{1/2} \quad (43)$$

These results are identical to the usual forms for free surface waves except for the function of  $\lambda_1$  and  $\lambda_2$  appearing in  $K_s$ ; the ice effect also enters through the definitions of  $k$  and  $C_{gr}$ .

Green (1978) presented results for normally incident waves shoaling on a plane beach. His results are identical to those presented here. A plot of shoaling coefficient  $K_s$  (with  $K_r = 1$  for normally incident waves) is given in Figure 1 for three different ice thicknesses along with the ice-free result. The results here were computed both with and without the ice acceleration effects in the wave dispersion relation. The results obtained for the two approximations were graphically indistinguishable, indicating the negligible effect of the ice mass on the wave properties. Results for obliquely incident waves were also obtained. The trend of results due to refraction at oblique incidence is essentially similar to the results for the ice-free case, and no further plots are included here.

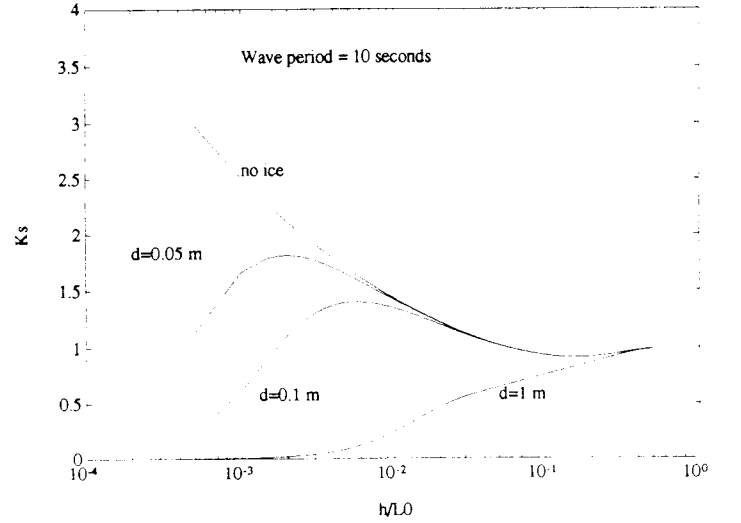


Figure 1: Shoaling coefficient  $K_s$  for waves shoaling over a plane beach (after Green, 1978).

## 4 A parabolic approximation

We now consider the development of a parabolic approximation for nearly unidirectional propagation under ice, following the work of Radder (1979) and others for surface water waves. The usual approach to this problem would be either to split the elliptic wave equation into forward and backward-propagating portions, as in Radder (1979), or to employ a WKB - type of expansion with spatial derivatives of coefficients and amplitudes handled in a multiple scale format. Since the wave-current model developed here is not conveniently written as a single governing equation, we take the somewhat unusual step of expanding the action and eikonal equations and then recombining them to obtain the parabolic approximation. (It is noted that the same results can be obtained using a direct multiple scale approach applied to the governing boundary value problem; see Kirby and Dalrymple (1983) or Kirby (1986).)

As usual, the ordering of spatial derivatives is handled using a multiple-scale approach. Taking  $\epsilon$  to characterise a small angular deviation between the direction of propagation and the  $x$  axis, we rewrite the phase function  $\psi$  defined in (30) as

$$\psi(\mathbf{x}) = \int k dx \mathbf{e}_x + \theta(\mathbf{x}) \quad (44)$$

The parabolic approximation arises from the assumption that  $\theta$  varies at a rate proportional to  $\epsilon$  in the  $y$  direction, but at a slower rate proportional to  $\epsilon^2$  in the  $x$  direction. At leading order, we then have

$$\mathbf{K} = (k + \epsilon^2 \theta_{X_2}) \mathbf{e}_x + \epsilon \theta_{Y_1} \mathbf{e}_y \quad (45)$$

$$|\mathbf{K}|^2 = k^2 + \epsilon^2 (2k\theta_{X_2} + (\theta_{Y_1})^2) + O(\epsilon^4) \quad (46)$$

$$\lambda_1^* = \lambda_1 + \epsilon^2 \frac{\lambda_1}{k^2} (2k\theta_{X_2} + (\theta_{Y_1})^2) + O(\epsilon^4) \quad (47)$$

$$\lambda_2^* = \lambda_2 + 2\epsilon^2 \frac{\lambda_2}{k^2} (2k\theta_{X_2} + (\theta_{Y_1})^2) + O(\epsilon^4) \quad (48)$$

$$\sigma^* = \omega - kU - \epsilon^2 (\theta_{X_2} U + \theta_{Y_1} V) = \sigma_1 - \epsilon^2 \sigma_2 \quad (49)$$

where it is assumed that the ambient current vector  $\mathbf{U} = (U, V)$  has a  $y$  direction component of  $O(\epsilon)$  relative to the  $x$  direction component. In order to maintain correspondence with the usual splitting matrix results, we take the variations of the ice layer and fluid domain to be

at most of  $O(\epsilon^2)$  in the  $x$  direction, but up to  $O(\epsilon)$  in the  $y$  direction. Using these approximations, we obtain the forms

$$\left[ \left( \frac{\sigma_1 a^2}{\sigma_0^2} \right) (C_g + U) \right]_{X_2} + \left[ \left( \frac{\sigma_1 a^2}{\sigma_0^2} \right) V \right]_{Y_1} + \left[ \frac{\theta_{Y_1}}{k} C_g \left( \frac{\sigma_1 a^2}{\sigma_0^2} \right) \right]_{Y_1} = 0 \quad (50)$$

for the transport equation, and

$$\begin{aligned} -2 \left[ \frac{\sigma_1}{\sigma_0^2} (C_g + U) \right] \theta_{X_2} a - 2 \left[ \frac{\sigma_1}{\sigma_0^2} V \right] \theta_{Y_1} a + \frac{\sigma_1}{\sigma_0^2} \left[ \frac{\sigma_0^2}{k \sigma_1} C_{g1} \left( \frac{\sigma_1 a}{\sigma_0^2} \right) \right]_{Y_1} \Big|_{Y_1} \\ + \left( \frac{2\lambda_2 - \lambda_1}{k^2} a_{Y_1} \right)_{Y_1} - \frac{\sigma_1}{k \sigma_0^2} C_g (\theta_{Y_1})^2 a = 0 \end{aligned} \quad (51)$$

for the eikonal equation. Here, subscripts  $X_2$  and  $Y_1$  represent slow spatial derivatives at the indicated order in powers of  $\epsilon$ . We introduce a complex amplitude  $\alpha$  given by

$$\eta = \alpha e^{i \int \bar{k} dx}, \quad \alpha = a e^{i \int (k - \bar{k}) dx + \theta} \quad (52)$$

where  $\bar{k}$  is some laterally averaged wavenumber which varies only in the  $x$  direction. After considerable algebra, the expressions (50) and (51) may be combined to give the parabolic approximation

$$\begin{aligned} (C_g + U) \alpha_{X_2} + V \alpha_{Y_1} + i (C_g + U) (\bar{k} - k) \alpha + \frac{\sigma_0^2}{\sigma_1} \\ \left( \left[ \frac{\sigma_1}{\sigma_0^2} (C_g + U) \right]_{X_2} + \left[ \frac{\sigma_1}{\sigma_0^2} V \right]_{Y_1} \right) \alpha - \frac{i}{2} \left[ \frac{\sigma_0^2}{k \sigma_1} C_g \left( \frac{\sigma_1 \alpha}{\sigma_0^2} \right) \right]_{Y_1} \Big|_{Y_1} = 0 \end{aligned} \quad (53)$$

This equation may be compared to the form given by Kirby (1986) for the case of wave-current interaction without ice (equation (55) there), and it is again apparent that a strong correspondence exists between the two models, aside from a single coefficient appearing in the diffraction term.

Two example calculations are presented here to illustrate several effects of ice on the wave propagation problem.

### 4.1 Wave diffraction by a circular ice lens

As a first example, we consider the effect of a finite region of relatively thick ice on waves propagating under an otherwise uniform ice sheet in water of constant depth. The lens has radius  $R$  and is centered at  $(x_0, y_0)$ . Outside the lens, the ice thickness is given by  $d_1$ . Inside the lens, the thickness varies according to

$$d(x, y) = d_1 + d_2 \left( 1 - \left( \frac{r}{R} \right)^2 \right); \quad r^2 = (x - x_0)^2 + (y - y_0)^2 \quad (54)$$

Results for one example are shown in Figure 2. For this case, we take the depth  $h = 10m$  and the uniform ice thickness  $d_1 = 0.5m$ . The ice lens has a radius  $R = 100m$  and an additional thickness  $d_2 = 1m$ . The wave period is 5 seconds. The figure shows contours of ice thickness as dashed lines, and contours of instantaneous surface elevation in increments of 0.25 times the incident wave height as solid lines. As waves propagating from left to right, they encounter the ice lens and experience a marked increase in phase speed. This causes wave crests to bend away from the lens region, directing the wave energy to the regions to either side of the lens. The local effect of the ice also causes a marked decrease in surface displacement amplitude, as in the shoaling examples in the previous section. Downwave of the ice lens, there is some recovery of the surface displacement amplitude as the ice thickness returns to its initial value, but the shadow zone created by the ice lens is dramatic and persists many wavelengths downwave of the localized disturbance. These results indicate that a localized region of ice with increased thickness or stiffness could provide a sheltering effect on structures or stretches of shoreline downwave of the obstacle.

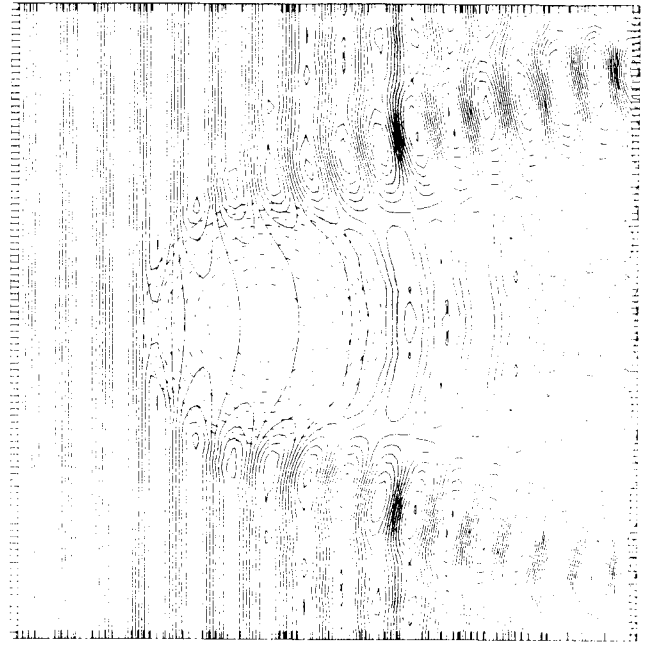


Figure 2: Diffraction of waves by a thick ice lens imbedded in a uniform ice sheet.

### 4.2 Effect of ice on wave diffraction by a shoal

As a second example, we study the effect of a uniform ice cover on a focussing and diffraction pattern caused by a local variation in water depth. The geometry studied is that of Berkhoff et al (1982); the experimental data from that study has been widely used as a verification test for combined refraction-diffraction computations. The details of the geometry are omitted for brevity.

Depth contours in increments of 5 cm are shown as dashed lines in Figures 3-4, with the elliptical feature representing a shoal which decreases the local depth. Figure 3 shows contours of an instantaneous surface, with contour increments of 0.5 times the incident wave amplitude. A focus and the development of a fringe pattern is apparent in the region downwave of the shoal, to the right in the picture. Also apparent is an area of increased wave height at the lower right corner of the domain. This effect is due to the presence of a reflecting lateral wall, which causes an area of increased wave height as waves are turned towards the wall by refraction.

In figure 4, surface contours are shown for the case where a uniform ice layer with a thickness of 1 cm (giving a  $\lambda_2$  value of 1.361 in deepwater for the 1 second wave considered here) covers the entire domain. The longer apparent wavelength reflects an increase in the wave phase speed resulting from bending effects in the ice. A focal region with relatively higher wave height is still apparent directly downwave of the shoal. However, the strength of the focus is quite weak relative to the ice free case. In addition, it is apparent that the wave height is initially decreased rather than increased as the waves begin to focus over the top of the shoal. This result is consistent with the general trend towards reduced wave heights during the shoaling process, as indicated in Figure 1.

## 5 Conclusions

The present paper has established a comprehensive framework for studying the propagation of waves under continuous sea ice in the finite-depth nearshore environment. In the linearized approximation, we have obtained the governing equations for waves in a domain in which depth, ambient current under the ice, and ice thickness, modulus and in-plane compressive stress are allowed to vary slowly relative



Figure 3: Surface contours, ice-free case. Geometry of Berkhoff et al (1982).

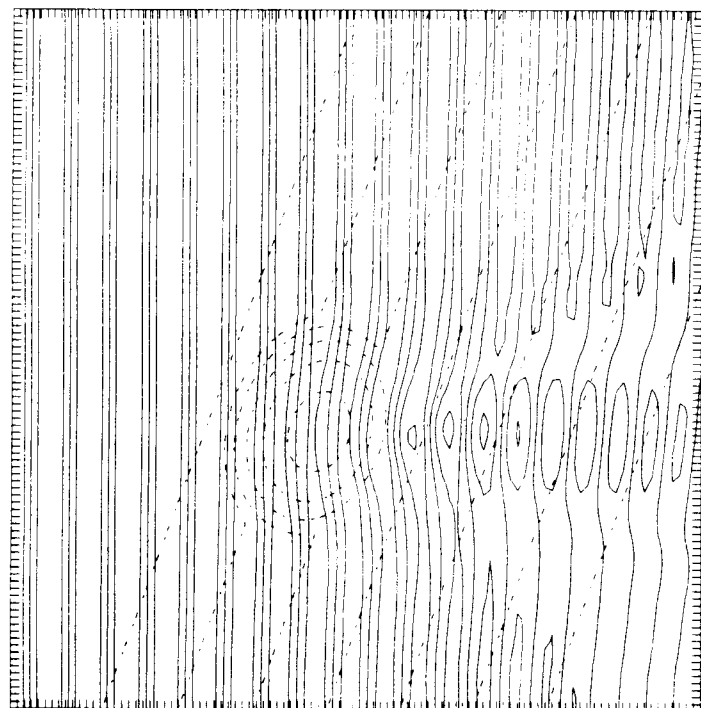


Figure 4: Surface contours, 1 cm uniform ice cover. Geometry of Berkhoff et al (1982).

to the wavelength. The wave action conservation law has been deduced for slowly-varying wave trains and has been shown to be identical to the result of Bretherton and Garrett (1969). The parabolic approximation has also been deduced and is found to be essentially the same as the wave-current model given by Kirby (1986), after some redefinition of the model coefficients. Examples have been provided which illustrate the effect of localized variations in ice thickness on the propagation of a plane wave, as well as the effect of an ice cover on processes controlled by localized variations in depth. The case of wave refraction under ice sheets with either isotropic compression or a general state of in-plane stress is likely to lead to results of interest and should be studied further.

In order to generalize the present model for detailed application to coastal wave climates, it will be necessary to obtain nonlinear extensions to the model formulations. An extension to finite depth of the results of Liu and Mollo-Christensen (1988) for narrow-banded Stokes waves would lead to evolution equations of cubic Schrodinger type in the parabolic approximation, as in Kirby and Dalrymple (1983) for surface waves alone. However, as pointed out by Green (1984), the ice-water system provides for the occurrence of resonant three-wave interactions, and so the nonlinear evolution of waves in the nearshore system may well be dominated by second-order interactions leading to significant modal energy exchanges, as in capillary-gravity wave systems. These effects remain to be investigated in detail.

#### Acknowledgements

This work is a result of research sponsored by NOAA Office of Sea Grant, Department of Commerce, under Grant No. NA/6RG0162-01 (Project No. R/OE-9). The U.S. Government is authorized to produce and distribute reprints for governmental purposes, notwithstanding any copyright notation that may appear hereon.

#### References

- Berkhoff, J. C. W., Booij, N. and Radder, A. C., 1982, "Verification of numerical wave propagation models for simple harmonic linear waves", *Coast. Engrng.* 6, 255-279.
- Bretherton, F. P. and Garrett, C. J. R., 1969, "Wavetrains in inhomogeneous moving media", *Proc. Roy. Soc. London A*, 302, 529-554.
- Green, T., 1978, "Shoaling of waves under ice", *J. Waterway, Port, Coast. and Ocean Engrng.*, 104, 327-330.
- Green, T., 1984, "The importance of nonlinear wave interactions under ice", *Proc. Hydraulics Spec. Conf, ASCE, Coeur d'Alene, Idaho*.
- Greenhill, A. G., 1887, "Wave motion in hydrodynamics", *Am. J. Maths.*, 9, 62-112.
- Keller, J. B. and Goldstein, E., 1953, "Water wave reflection due to surface tension and floating ice", *Trans. AGU*, 34, 43-48.
- Keller, J. B., 1958, "Surface waves on water of non-uniform depth", *J. Fluid Mech.*, 4, 607-614.
- Kerr, A. D., 1983, "The critical velocities of a load moving on a floating ice plate that is subjected to in-plane forces", *Cold Reg. Sci. Techn.*, 6, 267-274.
- Kheisin, D. Ye., 1967, *Dynamics of the Ice Cover*, Technical Translation FSTC-HT-23-485-69, U. S. Army Foreign Science and Technology Center, 258 p.
- Kirby, J. T. and Dalrymple, R. A., 1983, "A parabolic equation for the combined refraction-diffraction of Stokes waves by mildly varying topography", *J. Fluid Mech.*, 136, 453-466.

- Kirby, J. T., 1984, "A note on linear wave-current interaction over slowly-varying topography", *J. Geophys. Res.*, 89, 745-747.
- Kirby, J. T., 1986, "Higher-order approximations in the parabolic equation method for water waves", *J. Geophys. Res.*, 91, 933-952.
- Krasil'nikov, V. N., 1962, "Refraction of deflection waves", *Akusticheskiy Zhurnal AN SSSR*, 8(1) (as cited in Kheisin, 1967).
- Liu, A. K. and Mollo-Christensen, E., 1988, "Wave propagation in a solid ice pack", *J. Phys. Oceanogr.*, 18, 1702-1712.
- Love, A. E. H., 1944, *A Treatise on the Mathematical Theory of Elasticity*, Dover.
- Luke, J. C., 1967, "A variational principle for a fluid with a free surface", *J. Fluid Mech.*, 27, 395-397.
- Radder, A. C., 1979, "On the parabolic equation method for water-wave propagation", *J. Fluid Mech.*, 95, 159-176.
- Schulkes, R. M. S. M., Hosking, R. J. and Sneyd, A. D., 1987, "Waves due to a steadily moving source on a floating ice plate. Part 2", *J. Fluid Mech.*, 180, 297-318.
- Simmons, W. F., 1969, "A variational method for weak resonant wave interactions", *Proc. Roy. Soc. London*, A 309, 551-575.